Journal of Drug Delivery Science and Technology 59 (2020) 101918

Contents lists available at ScienceDirect

Journal of Drug Delivery Science and Technology

journal homepage: www.elsevier.com/locate/jddst

Antiinflammatory activity of carnauba wax microparticles containing curcumin

Bruno Ambrósio da Rocha [a,*], Cristhian Rafael Lopes Francisco [b], Mariana de Almeida [a], Franciele Queiroz Ames [a], Evandro Bona [b], Fernanda Vitória Leimann [b,c], Odinei Hess Gonçalves [b,c], Ciomar Aparecida Bersani-Amado [a]

[a] State University of Maringá (UEM), Department of Pharmacology and Therapeutics, Avenue Colombo, 5790, Jd. Universitário, 87020-900, Maringá, PR, Brazil
[b] Federal University of Technology – Paraná (UTFPR), Post-Graduation Program of Food Technology (PPGTA), POBox 271, BR 369, Km 0.5, 87301-006, Campo Mourão, PR, Brazil
[c] Centro de Investigação de Montanha (CIMO), Instituto Politécnico de Bragança, Campus de Santa Apolónia, 5300-253, Bragança, Portugal

ARTICLE INFO

Keywords:
Solid lipid microparticles
Carnauba wax
Curcumin
Inflammation
Food coloring

ABSTRACT

The pharmacokinetic of curcumin has posed a challenge to its therapeutic efficacy. Drug encapsulation systems, particularly microparticles, are promising due to their ability to protect compounds against both physical and chemical degradation and to improve their bioactivity. The aim of the present study was to prepare curcumin loaded solid lipid microparticles from carnauba wax and evaluate its antiinflammatory efficacy. Microparticles were obtained by hot homogenization technique and characterized by scanning electron microscopy, differential scanning calorimetry, infrared spectroscopy and X-ray diffraction demonstrating the effective encapsulation of curcumin. Antiinflammatory efficacy was evaluated comparing free curcumin and curcumin encapsulated by carrageenan-induced paw edema in rats. Additionally, myeloperoxidase (MPO) activity and concentration of nitric oxide (NO) were evaluated in plantar tissue of rats. Microparticles showed regular and spherical morphology with 20 μm diameter. Thermal, spectroscopic, X-ray and images analysis demonstrated the encapsulation of curcumin in the lipid matrix. The evaluation of antiinflammatory activity showed that encapsulated curcumin at doses of 25 and 50 mg kg^{-1} were more effective than free curcumin at lower doses of 25 and 50 mg. kg^{-1} and had similar efficacy to free curcumin at dose a 400 mg.kg^{-1}, inhibiting the development of edema, myeloperoxidase (MPO) activity, and the increase in nitric oxide (NO) levels. Overall, curcumin microparticles were obtained with high encapsulation efficiency and antiinflammatory efficacy 16-fold better than free curcumin.

1. Introduction

Curcumin is a polyphenolic compound obtained from *Curcuma longa* L. rhizomes [1] with demonstrated biological activity on various pathologies like rheumatoid arthritis, Alzheimer's disease, cancer [2–6] and as well as its natural antioxidant activity [7]. Curcumin is also a promising drug for the treatment of inflammatory diseases because of its ability to inhibit the expression of the enzyme cyclooxygenase 2 (COX2), to down regulate protein kinases, to inhibit the activation of nuclear factor κB (NF-κB), and to reduce the release of some proinflammatory cytokines and mediators, among other actions [4,5,8,9]. The suppression of prostaglandin synthesis [8] and reduction of metalloproteinase-3 from chondrocytes [4] are also known to be involved.

The unfavorable pharmacokinetics of curcumin need to be overcome to permit its therapeutic use. Encapsulation processes have been shown to be effective [10–13] and microparticles are promising candidates for the encapsulation of curcumin because of their low production cost and the ease to scale up. Curcumin has been encapsulated in PLLA [14], microemulsions [15] and solid lipid nano [16,17], and microparticles [18,19]. Lipid-based drug encapsulation systems comprise particles with a hydrophobic core that is stabilized by a superficial layer of surfactant, with the active compound immersed in the lipid matrix [20,21]. These systems present great bioavailability, the possibility of achieving modified release, the absence of organic solvents, a low production cost,

* Corresponding author. Department of Pharmacology and Therapeutics, State University of Maringá, Bloco K68, Avenue Colombo, 5790, Jd. Universitário, Maringá, 87020-900, Brazil.
E-mail address: brunoambrosiorocha@fai.com.br (B.A. Rocha).

https://doi.org/10.1016/j.jddst.2020.101918
Received 11 April 2020; Received in revised form 30 June 2020; Accepted 5 July 2020
Available online 16 July 2020

physicochemical stability, and protection of the active drug against degradation [22–24]. Low melting points lipids have been studied in encapsulation [25], but the use of high melting points materials as encapsulant such as carnauba wax is interesting because of the possible gains in stability when compared with to low melting point lipids. In this case, high temperatures are necessary in the particles production and a possible influence in curcumin activity is worth investigating. Carnauba wax, obtained from the carnauba palm tree, is a solid material having high melting temperatures [26,27]. It is composed of a complex blend of fatty esters, hydroxyacids and a small percentage of resins and offers a wide variety of applications in the industry and, particularly in the pharmaceutical industry, carnauba wax has gained interest due to its biocompatibility, low cost and sustained release of the drugs due to its high hydrophobicity [26,28,29].

Although the bioactivity of curcumin is well described in the literature, studies on the action of encapsulated curcumin are still a work in progress. The objective of the work was to obtain curcumin-loaded microparticles using carnauba wax as encapsulating material and to evaluate their antiinflammatory activity using a carrageenan-induced paw edema model. First, the characterization of the curcumin-loaded solid lipid microparticles was evaluated using different methodologies. Second, the activity of curcumin in its non-encapsulated form was compared to encapsulated curcumin in *in vivo* experiments.

2. Methodology

2.1. Materials

Carnauba wax, curcumin, medium-chain triglycerides (Miglyol® MCT; capric and caprylic acid triglycerides), and sodium caseinate were used to prepare the microparticles (all reagents were purchased from Sigma-Aldrich). Distilled water was used as the continuous medium for the preparation of the microparticles. Chloroform and methanol were acquired from common suppliers and used to characterize the microparticles. λ-Carrageenan was used as the phlogistic agent. Hydrogen peroxide, *o*-dianisidine and sodium acetate were used as reagents to determine myeloperoxidase (MPO) activity. Sulfanilamide and *N*-1-naphthylethylenediamine dihydrochloride were used to determine nitric oxide (NO) levels. All reagents were purchased from Sigma-Aldrich unless stated otherwise. Ortho-phosphoric acid (Nuclear, 85% purity) was used to determine NO.

2.2. Curcumin-loaded solid lipid microparticles

The curcumin-loaded solid lipid microparticles were obtained according to the method of Gonzalez-Mira et al. [30] with minor modifications. The aqueous phase was prepared by dissolving sodium caseinate (0.055 g) in water (50 g) and heating to 95 °C under gentle stirring. A jacketed borosilicate vessel was then connected to a thermostatic bath at 95 °C. MCT (2.000 g) and carnauba wax (3.000 g) were then added and allowed to melt. Then curcumin (0.1000 g) was added to the borosilicate vessel under gentle stirring and mixed for 5 min. The aqueous phase was then added under stirring using a high-efficiency stirrer (Ultra-Turrax IKA, T25) which was maintained for 15 min at 8000 rpm. At the end of this step, the dispersion was quickly cooled to solidify the particles and lyophilized. Finally, characterization and the evaluation of the acute antiinflammatory activity were carried out. Blank microparticles were obtained with the same materials and procedure but without curcumin.

2.3. Microparticles characterization

Encapsulation efficiency was evaluated in triplicate as follows. Approximately 5 ml of the dispersion of microparticles in water was washed with ethanol in a vacuum filter (3 μm porosity) to remove the surface, non-encapsulated curcumin. Particles were then oven dried at 60 °C for 2 h. The dried sample was placed in a test tube with 10 ml of dichloromethane and sealed. Samples were then stirred at room temperature for 24 h to extract the encapsulated curcumin. After this period, samples were filtered through an Amicon filter (Millipore, 100 kDa), and the concentration of encapsulated curcumin ($[cur]_{encapsulated}$) was determined by UV–Vis spectroscopy at 427 nm [21]. The same procedure was performed for the unwashed microparticles to determine the total amount of curcumin present (both encapsulated and non-encapsulated, $[cur]_{total}$). Encapsulation efficiency (EE%) was determined by Equation (1).

$$EE\% = 100\ x\ \left(\frac{[cur]_{encapsulated}}{[cur]_{total}}\right) \quad (1)$$

Curcumin load in the microparticles ($mg_{cur}.g^{-1}_{particles}$), representing the concentration of curcumin inside the microparticles, was determined by Equation (2). The mass of the microparticles ($m_{particles}$) and curcumin that was effectively encapsulated (m_{cur}) were determined spectrophotometrically as described above.

$$Curcumin\ load\ = 100\ x\ EE\ x\ \frac{m_{cur}}{m_{particles}} \quad (2)$$

Scanning electron microscopy (Shimadzu, SS550) images were used to measure the microparticles diameter and to evaluate the morphology of curcumin and microparticles. The average particles diameter (Dz) was determined as an arithmetic average. Coefficient of variation of the diameters (CV; dimensionless) was determined by Equation (3) using the standard deviation of the diameters (SD). At least 250 microparticles were measured.

$$CV(-) = \frac{SD}{Dz} \quad (3)$$

Differential scanning calorimetry (Perkin Elmer model 4000) was used to evaluate the physical state of curcumin after the encapsulation procedure. Approximately 10 mg of each sample was placed in an aluminum holder and heated from 0 to 390 °C at 20 °C.min^{-1}, with a nitrogen flow rate of 50 ml min^{-1}. X-ray diffractograms of carnauba wax, curcumin, physical mixture (carnauba wax and curcumin manually mixed in the same proportions found in the microparticles), blank microparticles (no curcumin added) and the curcumin-loaded microparticles were obtained using an X-ray diffractometer (LabX model XRD-6000, Shimadzu, Japan) from 2° to 60° at 6° min^{-1}. Fourier transform infrared spectroscopy (Frontier PerkinElmer) was performed with Attenuated Total Reflectance (ATR) at a resolution of 2 cm^{-1} from 4000 to 600 cm^{-1} in triplicate. All spectra were normalized to allow proper comparison. The morphology of the microparticles was evaluated by scanning electron microscopy (Shimadzu, SS550) using secondary electrons for detection. Samples were gold coated before analyses. When necessary, a physical mixture of curcumin and carnauba wax were obtained by manually mixed them in a crucible then in the same proportion of the microparticles.

2.4. Animals and treatments

Male Wistar rats weighing 200–220 g and housed at 22 °C under a 12 h/12 h light/dark cycle with food and water available *ad libitum* were used. Curcumin (Cur) and curcumin-loaded microparticles (SLMCur) were dispersed in water and orally administered in a single daily dose 1 h prior to the induction of the inflammatory response. Cur was administered at doses of 25, 50, and 400 mg.kg^{-1} while SLMCur was administered at doses of 25 and 50 mg.kg^{-1} as previously described [13]. The experimental protocol was approved by the Committee on Ethics in the Use of Animals under the number CEUA no. 6811200515.

2.5. Carrageenan-induced paw edema

Rats ($n = 6$ per group) received an intraplantar injection of 100 μl of carrageenan (Cg) solution in the left hind paw (200 μg/paw). The right

contralateral paw was injected with the same volume of vehicle (0.9% saline solution). The volume of both paws was determined 1, 2, and 4 h after the carrageenan injection using a digital plethysmograph. The increase in paw volume (edema) was calculated by subtracting the volume of the contralateral paw that received saline solution from the volume of the left paw that received Cg solution.

2.6. Myeloperoxidase activity and nitrite concentration

Rats were anesthetized and euthanized 4 h after the paw edema induction. The plantar tissue was removed, placed in an eppendorf tube that already contained phosphate-buffered saline, homogenized, and centrifuged [13]. Myeloperoxidase activity was determined in the supernatant of the homogenate in duplicate. Samples (10 μl) were placed in a 96-well microplate and a solution of *o*-dianisidine was added. After 5 min, the reaction was stopped using sodium acetate solution, and MPO activity was determined by the endpoint technique using absorbance analysis at 450 nm. Data are expressed as optical density (OD).

The concentration of nitrite oxide (NO) was determined by the Griess technique, which indirectly determines the concentration of nitrite in the tissue samples. The supernatant (50 μl) of plantar tissue was placed in a 96-well microplate in triplicate, and Griess solution was added at room temperature. After 10 min, the microplate was read at 550 nm using an enzyme-linked immunosorbent assay reader as described previously [31]. Nitrite oxide concentration was calculated as the mean of a sodium nitrite standard curve and results are expressed in μM.

2.7. Statistical analysis

For the biological response data, results were expressed as mean ± standard error of the mean (SEM) and were evaluated using analysis of variance (ANOVA) followed by the Tukey test. Values of $p < 0.05$ were considered statistically significant.

3. Results and discussion

3.1. Characterization of the curcumin-loaded solid lipid microparticles

Table 1 shows encapsulation efficiency, curcumin load in the microparticles, average diameter, and coefficient of variation of diameters. Fig. 1 presents the scanning electron microscopy images of pure curcumin, physical mixture (carnauba wax and curcumin manually mixed in a crucible in the same proportion of the microparticles), curcumin-loaded microparticles and blank microparticles (no curcumin added).

Curcumin appeared as regular particles which is characteristic of its highly crystalline microstructure and with sizes of less than 20 μm. In the physical mixture images, one may see that carnauba wax is composed of irregular particles with sizes ranging from 100 μm to less than 10 μm. Curcumin crystals are also visible in these images. Microparticles (both blank and curcumin-loaded) presented regular, spherical morphology with diameters around 20 μm with no fissures or surface irregularities. Images show no free curcumin crystals in the microparticles images, which is indicative that curcumin is not located outside the particles as free crystals. Silva-Buzanello et al. [32] performed scanning electron microscopy of curcumin-loaded PLLA nanoparticles and observed free curcumin crystals in the cases where low encapsulation efficiencies were detected.

Microparticles presented high encapsulation efficiency which may be explained by the hydrophobic character of the lipids used as encapsulants and curcumin. Efficiency is mostly dependent on the interactions between encapsulant and encapsulated compounds and also on the encapsulation technique used. High efficiencies were found for gelatin-curcumin complexes (97%) [33], whey protein isolate (95–97%) [34], while efficiencies from 90 to 30% were found in supercritical processes [19]. Incorporation of curcumin in solid lipid nanoparticles were also investigated and efficiencies ranged from 47 to 90% depending on the experimental conditions and encapsulant used [16].

Table 1
Encapsulation efficiency (EE), curcumin load in the microparticles, average diameter (Dz) and coefficient of variation of the diameters (CV).

EE (%)	Load (mg_{cur}/g_{part})	Dz (μm)	CV(−)
81.7 ± 1.6	15.9 ± 0.1	20.0 ± 2.0	0.41

Figs. 2–4 present the X-ray diffractograms, the FTIR spectra, and the DSC thermograms, respectively. Table 2 presents the melting temperature and melting enthalpy of the lipid encapsulants.

X-ray diffraction analyses revealed peaks at 21.5° and 23.8° for blank microparticles, which are representative of short spacing and indicate the side-by-side orientation of hydrocarbon chains of the partially crystalline structure [35]. For pure curcumin, peaks were detected at 8.9°, 9.7°, 12.2°, 13°, 14.6°, 17.3°, and 19.5°, corresponding to its crystalline structure [36–38]. Such peaks were not visualized in curcumin-loaded microparticles, but they were found in the physical mixture. This indicates that curcumin in the microparticles was located inside the lipid matrix forming a solid solution in an amorphous state. The decrease in the curcumin crystalline behavior after encapsulation strongly suggests its efficient encapsulation.

A decrease in the lipid crystallinity is observed in the region of 2θ between 15° and 20° in the blank and curcumin-loaded microparticles. It was not observed in the physical mixture sample which may be attributed to the presence of MCT in the formulation of the microparticles [27,39]. Lipid crystallinity is a determining factor in the process of drug encapsulation, since a highly crystalline state may lead to non-entrapment of the drug while disorder in the crystalline structure favors encapsulation. This shoulder between 15° and 20° is even more pronounced in the curcumin-loaded microparticles indicating that the presence of curcumin led to a higher disorder in the lipid structure.

FTIR analyses of curcumin revealed axial stretching absorption bands of the OH group at 3510 cm^{-1}, which is often used to evaluate interactions between curcumin and encapsulants [40,41]. This absorption band was evident in samples that contained curcumin and the physical mixture of curcumin and carnauba wax. However, the same was not observed in samples of curcumin-loaded microparticles and blank microparticles.

Thermal analysis showed that the melting point of curcumin was 173.6 °C, which is consistent with previous studies [41–43]. In the curcumin-loaded microparticles the melting peak of curcumin was not detected indicating that it is in amorphous state. The physical mixture, the melting peak of curcumin was not detected which was likely due to its low concentration in the samples. The melting point of carnauba wax in the microparticles was slightly lower than the melting point in the physical mixture, which may be attributable to the absence of MCT, which is a liquid and causes the decrease in the crystallinity of the carnauba wax [44]. The presence of curcumin in the microparticles also led to a decrease in the melting temperature, suggesting that curcumin hindered the formation of crystalline domains of the carnauba wax during particles solidification. The influence of MCT and curcumin was more evident in the melting enthalpy of the lipid phase since an accentuated decrease was detected caused by the presence of curcumin. This is also a strong indicative of curcumin encapsulation in the lipid matrix.

Characterization analyses agreed that curcumin was efficiently encapsulated inside the lipid matrix meaning that the microencapsulation system composed by solid and liquid lipid matrix together with the hot homogenization technique is suitable to obtain curcumin-loaded microparticles. The high encapsulation efficiency and the narrow size distribution make then excellent candidates for *in vivo* studies.

3.2. Antiinflammatory activity

Fig. 5 shows the antiinflammatory activity of free curcumin (Cur)

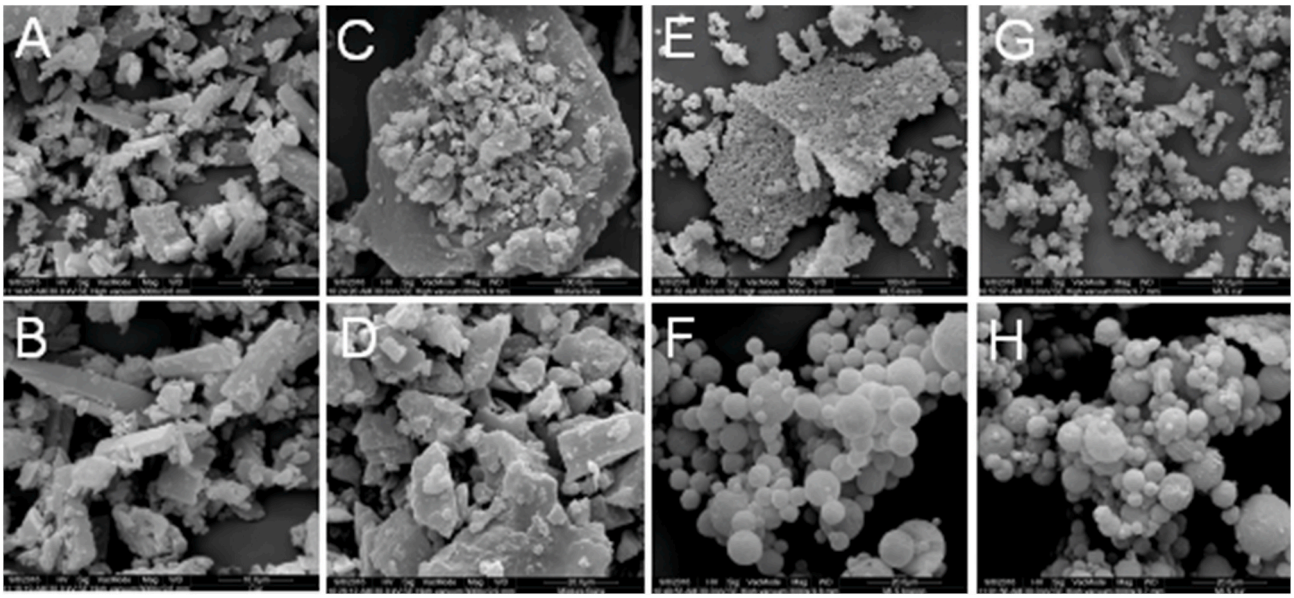

Fig. 1. Micrographs of curcumin (A and B); physical mixture of carnauba wax and curcumin (C and D); blank solid lipid microparticles (no curcumin added, E and F) and curcumin-loaded solid lipid microparticles (G and H).

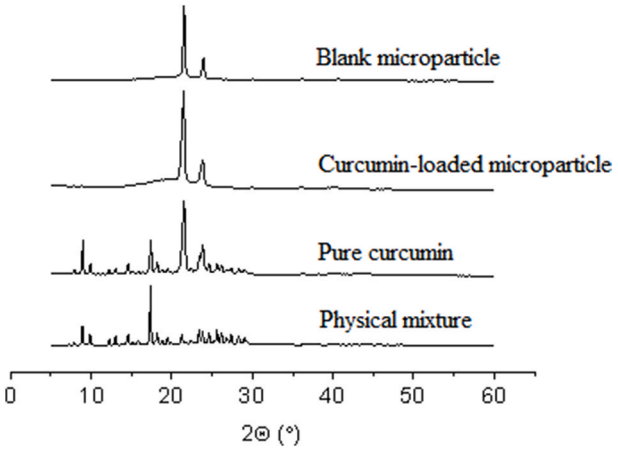

Fig. 2. X-ray diffraction patterns of blank solid lipid microparticles (no curcumin added), curcumin-loaded solid lipid microparticles, curcumin and physical mixture (carnauba wax and curcumin manually mixed).

and the curcumin-loaded microparticles (SLMCur), presenting the development of paw edema in rats, myeloperoxidase (MPO) activity and nitrite concentration in the supernatant of the plantar tissue of each group.

The experimental model of induced paw edema by carrageenan (Cg) presented an inflammatory process with maximum intensity 4 h after the carrageenan injection, characterized by erythema, hyperalgesia, and edema resulting from the release of numerous proinflammatory mediators, such as histamine, bradykinin, prostaglandins, reactive oxygen species, reactive nitrogen species, and cytokines [45–47].

In this experimental model, free curcumin treatment at a dose of 400 $mg.kg^{-1}$ significantly reduced (by 24.2%) the formation of edema 4 h after the carrageenan injection. Lower doses of free curcumin (25 and 50 $mg.kg^{-1}$) did not inhibit the formation of edema (Fig. 5A). Treatment with the curcumin-loaded solid lipid microparticles (SLMCur) at 25 and 50 $mg.kg^{-1}$ significantly inhibited (by 18.2% and 32.5%, respectively) the development of edema 4 h after the carrageenan injection (Fig. 5B). Treatment with SLMCur at a dose of 50 $mg.kg^{-1}$ was more effective than treatment with 400 $mg.kg^{-1}$ and significantly better than free curcumin treatment at doses of 25 and 50 $mg.kg^{-1}$.

The antiinflammatory effect may be at least partially explained by inhibitory effects on the synthesis or release of inflammatory mediators [45–47]. Four hours after induction of the inflammatory response, nitrite concentration increased. Treatment with SLMCur at 25 and 50 $mg.kg^{-1}$ significantly inhibited nitrite levels by 39.9% and 42.1%, respectively, compared with the carrageenan group (Fig. 5D). However, no dose of free curcumin inhibited the increase in nitrite concentration.

During the development of the inflammatory process induced by carrageenan, intense cellular recruitment occurs, which may be indirectly observed as an increase in myeloperoxidase (MPO) activity. Treatment with free curcumin at the highest tested dose (400 $mg.kg^{-1}$) and SLMCur at 25 and 50 $mg.kg^{-1}$ significantly inhibited MPO activity by 42.2%, 33.7%, and 36.2%, respectively, when compared with the carrageenan group (Fig. 5C).

The antiinflammatory activity of curcumin involves the inhibition of the enzyme cyclooxygenase 2 and NF-κB and the reduction of the synthesis/release of proinflammatory mediators, such as cytokines and free radicals that are derived from oxygen and nitrogen [8,9,48]. However, the pharmacological effects of curcumin may only be achieved if pharmacologically active plasma and tissue concentrations are attained. In this context, results suggest that the bioavailability of curcumin may be improved when it is orally administered as loaded microparticles, since lower doses of encapsulated curcumin had better efficacy than free curcumin. The increase in the bioavailability of curcumin and plasma levels in curcumin-loaded microemulsions was already confirmed [15].

This hypothesis is supported by previous studies. Microencapsulation of ketoprofen in carnauba wax showed that sustained release of the active substance lasted more than 24 h *in vitro* [26]. Additionally, it was demonstrated that the way in which the concentration of carnauba wax is increased the release of the active agent becomes prolonged and sustained [49]. The sustained release of curcumin when encapsulated in carnauba wax may be explained by the fact that carnauba wax is very lipophilic and usually contains natural resins, which prevents the entry of water into the lipid structure. It also presents low concentration of free fatty acids and hydroxyl groups, which delay its degradation and so the release of the encapsulated drug [29,49].

Recently, it was demonstrated that curcumin-loaded PLLA (poly-L-lactic acid) nanoparticles showed an antiinflammatory efficacy with doses eight times lower than free curcumin [13]. Cai et al. [50] showed

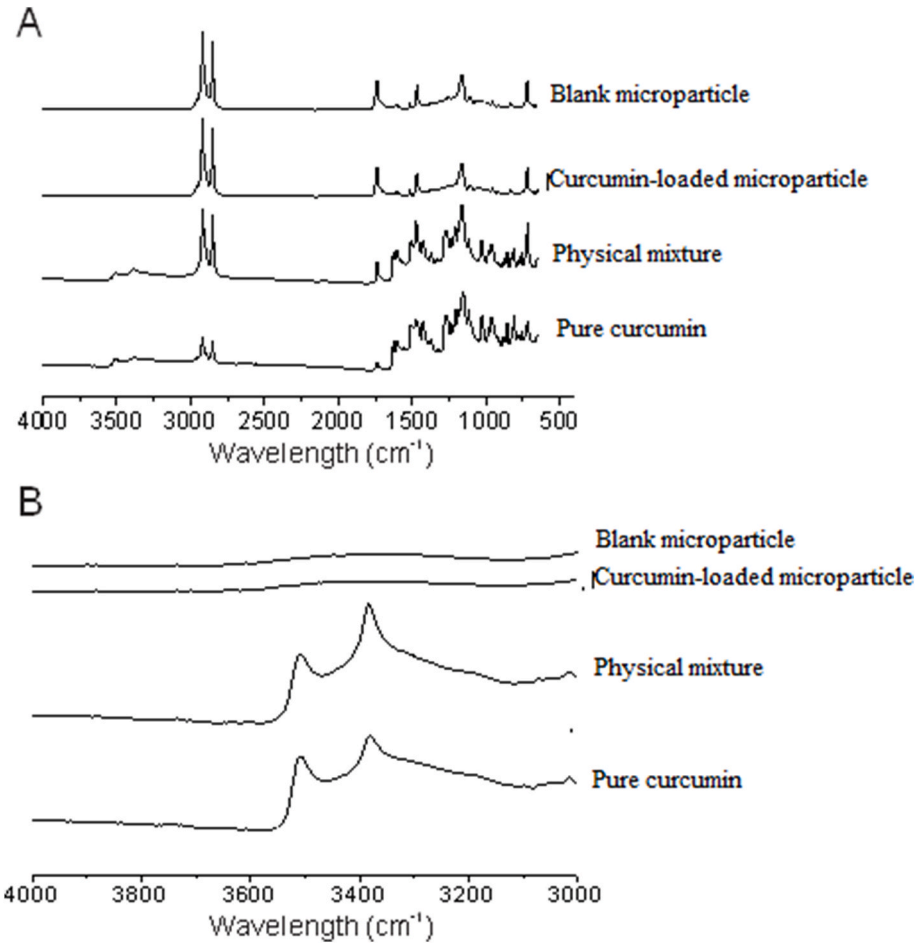

Fig. 3. FTIR spectra of blank solid lipid microparticles (no curcumin added), curcumin-loaded solid lipid microparticles, curcumin and physical mixture (carnauba wax and curcumin manually mixed).

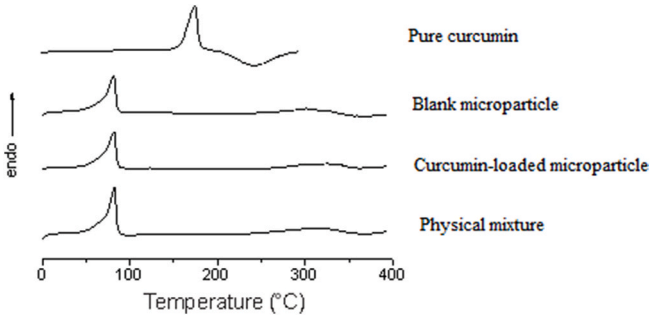

Fig. 4. DSC thermograms of blank solid lipid microparticles (no curcumin added), curcumin-loaded solid lipid microparticles, curcumin and physical mixture (carnauba wax and curcumin manually mixed).

Table 2
Melting temperature and melting enthalpy of the lipid encapsulant in the curcumin-loaded solid lipid microparticles, blank solid lipid microparticles (no curcumin added) and physical mixture (carnauba wax and curcumin manually mixed).

Sample	$T_{lipid\ fusion}$ (°C)	$\Delta H_{lipid\ fusion}$ (J.g^{-1})
Physical mixture	82.2	167
Blank microparticles	81.7	164
Curcumin-loaded microparticles	81.3	134

that a curcumin nanoformulation improved curcumin uptake threefold when compared to curcumin suspension and still showed antiinflammatory efficacy in the adjuvant-induced arthritis model.

4. Conclusion

Microparticles were obtained by the hot homogenization technique, presenting average diameter of 20 μm with no visible free curcumin crystals. High encapsulation efficiency was found and thermal, spectroscopic and X-ray analyses confirmed that curcumin existed as an amorphous material inside the microparticles. The encapsulated curcumin demonstrated better antiinflammatory efficacy than free curcumin since concentrations of 16-fold lower doses.

Author statement

Bruno Ambrósio da Rocha: Conceptualization, Investigation, Methoology, Roles/Writing – original draft, Writing – review & editing. **Cristhian Rafael Lopes Francisco:** Investigation. **Mariana de Almeida:** Investigation. **Franciele Queiroz Ames:** Investigation. **Evandro Bona:** Methodology. **Fernanda Vitória Leimann:** Conceptualization, Methodology. **Odinei Hess Gonçalves:** Conceptualization, Methodology, Project administration, Funding acquisition, Resources, Roles/Writing – original draft, Writing – review & editing. **Ciomar Aparecida Bersani-Amado:** Conceptualization, Methodology, Project administration, Funding acquisition, Resources, Roles/Writing – original draft, Writing – review & editing.

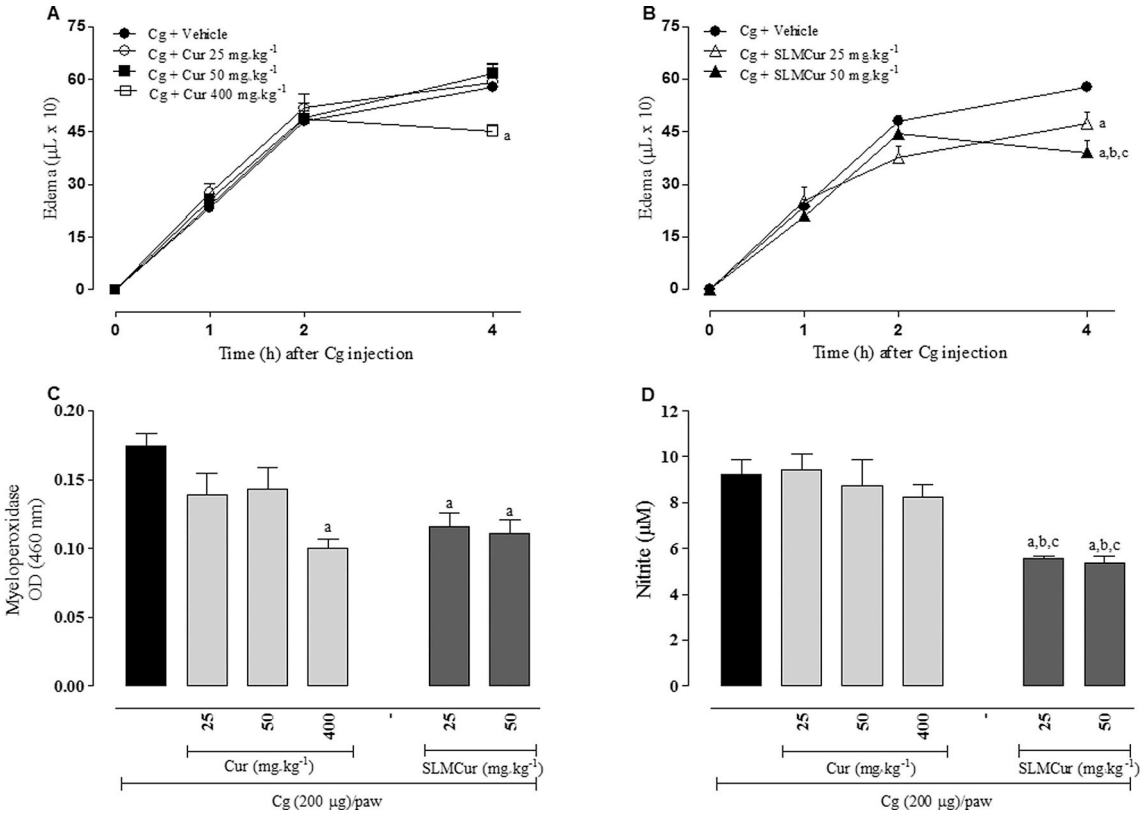

Fig. 5. Effect of free curcumin (Cur) and curcumin-loaded solid lipid microparticles (SLMCur) on the development of paw edema induced by intraplantar injection of carrageenan (Cg 200 µg/paw) in rats (200–220 g). (A) Animals (n = 6 per group) treated with Cur (*per* oral) at doses 25, 50 and 400 mg.kg^{-1}; (B) animals (n = 6 per group) treated with SLMCur orally at doses 25 and 50 mg.kg^{-1}. Each point represents mean ± SEM of the paw volume 1, 2 and 4 h after Cg injection. (C, D) Myeloperoxidase (MPO) and nitrite concentration (NO) in the supernatant of the plantar tissue of each group after the fourth hour of Cg injection. a $P<0.01$ compared to Cg group. b $P < 0.01$ compared to Cur_{25} group. c $P < 0.01$ compared to Cur_{50} group (ANOVA, Tukey's test).

Declaration of competing interest

The authors declare that they have no known competing financial interests or personal relationships that could have appeared to influence the work reported in this paper.

Acknowledgements

Authors thank CAPES, CNPq and Fundação Araucária for the support.

Appendix A. Supplementary data

Supplementary data to this article can be found online at https://doi.org/10.1016/j.jddst.2020.101918.

References

[1] V.B. Liju, K. Jeena, R. Kuttan, An evaluation of antioxidant, anti-inflammatory, and antinociceptive activities of essential oil from Curcuma longa, L., Indian J. Pharmacol. 43 (5) (2011) 526–531, https://doi.org/10.4103/0253-7613.84961.
[2] S. Ganta, M. Amiji, Coadministration of paclitaxel and curcumin in nanoemulsion formulations to overcome multidrug resistance in tumor cells, Mol. Pharm. 6 (3) (2009) 928–939, https://doi.org/10.1021/mp800240j.
[3] A.B. Kunnumakkara, P. Anand, B.B. Aggarwal, Curcumin inhibits proliferation, invasion, angiogenesis and metastasis of different cancers through interaction with multiple cell signaling proteins, Canc. Lett. 269 (2) (2008) 199–225, https://doi.org/10.1016/j.canlet.2008.03.009.
[4] M. Mathy-Hartert, I. Jacquemond-Collet, F. Priem, C. Sanchez, C. Lambert, Y. Henrotin, Curcumin inhibits pro-inflammatory mediators and metalloproteinase-3 production by chondrocytes, Inflamm. Res. 58 (12) (2009) 899–908, https://doi.org/10.1007/s00011-009-0063-1.
[5] C. Park, D.O. Moon, I.W. Choi, B.T. Choi, T.J. Nam, C.H. Rhu, T.K. Kwon, W.H. Lee, G.Y. Kim, Y.H. Choi, Curcumin induces apoptosis and inhibits prostaglandin E(2) production in synovial fibroblasts of patients with rheumatoid arthritis, Int. J. Mol. Med. 20 (3) (2007) 365–372, https://doi.org/10.3892/ijmm.20.3.365.
[6] X. Zhang, H. Zhang, L. Si, Y. Li, Curcumin mediates presenilin-1 activity to reduce beta-amyloid production in a model of Alzheimer's disease, Pharmacol. Rep. 63 (5) (2011) 1101–1108.
[7] J. Wu, X. Sun, X. Guo, M. Ji, J. Wang, C. Cheng, L. Chen, C. Wen, Q. Zhang, Physicochemical, antioxidant, in vitro release, and heat sealing properties of fish gelatin films incorporated with β-cyclodextrin/curcumin complexes for apple juice preservation, Food Bioprocess Technol. 11 (2) (2018) 447–461, https://doi.org/10.1007/s11947-017-2021-1.
[8] A. Goel, C.R. Boland, D.P. Chauhan, Specific inhibition of cyclooxygenase-2 (COX-2) expression by dietary curcumin in HT-29 human colon cancer cells, Canc. Lett. 172 (2) (2001) 111–118, https://doi.org/10.1016/s0304-3835(01)00655-3.
[9] C. Jobin, C.A. Bradham, M.P. Russo, B. Juma, A.S. Narula, D.A. Brenner, R. B. Sartor, Curcumin blocks cytokine-mediated NF-kB activation and proinflammatory gene expression by inhibiting inhibitory factor I-kB kinase activity, J. Immunol. 163 (1999) 3474–3483.
[10] P.N. Ezhilarasi, P. Karthik, N. Chhanwal, Nanoencapsulation techniques for food bioactive components: a review, Food Bioprocess Technol. 6 (2013) 628–647, https://doi.org/10.1007/s11947-012-0944-0.
[11] N.K. Gupta, V.K. Dixit, Bioavailability enhancement of curcumin by complexation with phosphatidyl choline, J. Pharmaceut. Sci. 100 (5) (2011), https://doi.org/10.1002/jps.22393, 1987–1995.
[12] S.K. Jain, M.S. Gill, H.S. Pawar, S. Suresh, Novel curcumin diclofenac conjugate enhanced curcumin bioavailability and efficacy in streptococcal cell wall-induced arthritis, Indian J. Pharmaceut. Sci. 76 (5) (2014) 415–422.
[13] B.A. Rocha, O.H. Gonçalves, F.V. Leimann, E.S.W. Rebecca, R.A. Silva-Buzanello, L. C. Filho, P.H.H. Araújo, R.K.N. Cuman, C.A. Bersani-Amado, Curcumin encapsulated in poly-L-lactic acid improves its anti-inflammatory efficacy in vivo, Adv. Med. Plant Res. 2 (4) (2014) 62–73.
[14] R.A. Silva-Buzanello, A.C. Ferro, E. Bona, L. Cardozo-Filho, P.H.H. Araújo, F. V. Leimann, O.H. Gonçalves, Validation of an Ultraviolet-visible (UV-Vis) technique for the quantitative determination of curcumin in poly(l-lactic acid) nanoparticles, Food Chem. 172 (2015) 99–104, https://doi.org/10.1016/j.foodchem.2014.09.016.
[15] Y. Xiao, X. Chen, L. Yang, X. Zhu, L. Zou, F. Meng, Q. Ping, Preparation and oral bioavailability study of curcuminoid-loaded microemulsion, J. Agric. Food Chem. 61 (15) (2013) 3654–3660, https://doi.org/10.1021/jf400002x.

[16] J. Sun, C. Bi, H.M. Chan, S. Sun, Q. Zhang, Y. Zheng, Curcumin-loaded solid lipd nanoparticles pronlonged in vitro antitumour activity, cellular uptake and improved in vivo bioavailability, Colloids Surf. B Biointerfaces 111 (2013) 367–375, https://doi.org/10.1016/j.colsurfb.2013.06.032.
[17] T. Wang, X. Ma, Y. Lei, Y. Luo, Solid lipid nanoparticles coated with cross-linked polymeric double layer for oral delivery of curcumin, Colloids Surf. B Biointerfaces 148 (2016) 1–11, https://doi.org/10.1016/j.colsurfb.2016.08.047.
[18] A. Bucurescu, A.C. Blaga, B.N. Estevinho, F. Rocha, Microencapsulation of curcumin by a spray-drying technique using gum Arabic as encapsulating agent and release studies, Food Bioprocess Technol. 11 (10) (2018) 1795–1806, https://doi.org/10.1007/s11947-018-2140-3.
[19] A.S. Pedro, S.D. Villa, P. Caliceti, S.A.B.V. De Melo, E.C. Albuquerque, A. Bertucco, S. Salmaso, Curcumin-loaded solid lipid particles by PGSS technology, J. Supercrit. Fluids 107 (2016) 534–541, https://doi.org/10.1016/j.supflu.2015.07.010.
[20] S. Jaspart, G. Piel, L. Delattre, B. Evrard, Solid lipid microparticles: formulation, preparation, characterisation, drug release and applications, Expet Opin. Drug Deliv. 2 (1) (2005) 75–87, https://doi.org/10.1517/17425247.2.1.75.
[21] W. Mehnert, K. Mäder, Solid lipid nanoparticles: production, characterization and applications, Adv. Drug Deliv. Rev. 47 (2001) 165–196, https://doi.org/10.1016/s0169-409x(01)00105-3.
[22] A. Dalpiaz, M. Mezzena, A. Scatturin, S. Scalia, Solid lipid microparticles for the stability enhancement of the polar drug N6-cyclopentyladenosine, Int. J. Pharm. 355 (2008) 81–86, https://doi.org/10.1016/j.ijpharm.2007.11.044.
[23] M. Mezzena, S. Scalia, P.M. Young, D. Traini, Solid lipid budesonide microparticles for controlled release inhalation therapy, AAPS J. 11 (4) (2009) 771–778, https://doi.org/10.1208/s12248-009-9148-6.
[24] R. Tursilli, G. Piel, L. Delattre, S. Scalia, Solid lipid microparticles containing the sunscreen agent, octyl-dimethylaminobenzoate: effect of the vehicle, Eur. J. Pharm. Biopharm. 66 (3) (2007) 483–487, https://doi.org/10.1016/j.ejpb.2007.02.017.
[25] M. Li, M.R. Zahi, Q. Yuan, F. Tian, H. Liang, Preparation and stability of astaxanthin solid lipid nanoparticles based on stearic acid, Eur. J. Lipid Sci. Technol. 118 (4) (2016) 592–602, https://doi.org/10.1002/ejlt.201400650.
[26] R.B. Oliveira, T.L. Nascimento, E.M. Lima, Design and characterization of sustained release ketoprofen entrapped carnauba wax microparticles, Drug Dev. Ind. Pharm. 38 (1) (2012) 1–11, https://doi.org/10.3109/03639045.2011.587433.
[27] J.R. Villalobos-Hernández, C.C. Müller-Goymann, Novel nanoparticulate carrier system based on carnauba wax and decyl oleate for the dispersion of inorganic sunscreens in aqueous media, Eur. J. Pharm. Biopharm. 60 (1) (2005) 113–122, https://doi.org/10.1016/j.ejpb.2004.11.002.
[28] J. Milanovic, S. Levic, V. Manojlovic, V. Nedovic, B. Bugarski, Carnauba wax microparticles produced by melt dispersion technique, Chem. Pap. 65 (2) (2011) 213–220, https://doi.org/10.2478/s11696-011-0001-x.
[29] M. Özyazici, E.H. Gökçe, G. Ertan, Release and diffusional modeling of metronidazole lipid matrices, Eur. J. Pharm. Biopharm. 63 (3) (2006) 331–339, https://doi.org/10.1016/j.ejpb.2006.02.005.
[30] E. Gonzalez-Mira, M.A. Egea, E.B. Souto, A.C. Calpena, M.L. Garc, Optimizing flurbiprofen-loaded NLC by central composite factorial design for ocular delivery, Nanotechnology 22 (4) (2011), https://doi.org/10.1088/0957-4484/22/4/045101, 045101.
[31] T.S. Saleh, J.B. Calixto, Y.S. Medeiros, Effects of anti-inflammatory drugs upon nitrate and myeloperoxidase levels in the mouse pleurisy induced by carrageenan, Peptides 20 (8) (1999) 949–956, https://doi.org/10.1016/s0196-9781(99)00086-8.
[32] R.A. Silva-Buzanello, M.F. Souza, D.A. Oliveira, E. Bona, F.V. Leimann, L.C. Filho, P.H.H. Araújo, S.R.S. Ferreira, O.H. Gonçalves, Preparation of curcumin-loaded nanoparticles and determination of the antioxidant potential of curcumin after encapsulation, Polímeros 26 (3) (2016) 207–214, https://doi.org/10.1590/0104-1428.2246.
[33] J. Gómez-Estaca, M.P. Balaguer, G. López-Carballo, R. Gavara, P. Hernández-Muñoz, Improving antioxidant and antimicrobial properties of curcumin by means of encapsulation in gelatin through electrohydrodynamic atomization, Food Hydrocolloids 70 (2017) 313–320, https://doi.org/10.1016/j.foodhyd.2017.04.019.
[34] W. Liu, X.D. Chen, Z. Cheng, C. Selomulya, On enhancing the solubility of curcumin by microencapsulation in whey protein isolate via spray drying, J. Food Eng. 169 (2016) 189–195, https://doi.org/10.1016/j.foodhyd.2017.04.019.
[35] I. Donhowe, O. Fennema, Water vapour and oxygen permeability of wax films, J. Am. Oil Chem. Soc. 70 (9) (1993) 867–873, https://doi.org/10.1007/BF02545345.
[36] I.S. Bayer, D. Fragouli, P.J. Martorana, L. Martiradonna, R. Cingolani, A. Athanassiou, Solvent resistant superhydrophobic films from self-emulsifying carnauba wax-alcohol emulsions, Soft Matter 7 (18) (2011) 7939–7943, https://doi.org/10.1039/C1SM05710C.
[37] C.S. Mangolim, C. Moriwaki, A.C. Nogueira, F. Sato, M.L. Baesso, A.M. Neto, G. Matioli, Curcumin-β-cyclodextrin inclusion complex: stability, solubility, characterisation by FT-IR, FT-Raman, X-ray diffraction and photoacoustic spectroscopy, and food application, Food Chem. 153 (2014) 361–370, https://doi.org/10.1016/j.foodchem.2013.12.067.
[38] J.R. Villalobos-Hernández, C.C. Müller-Goymann, Sun protection enhancement of titanium dioxide crystals by the use of carnauba wax nanoparticles: the synergistic interaction between organic and inorganic sunscreens at nanoscale, Int. J. Pharm. 322 (2006) 161–170, https://doi.org/10.1016/j.ijpharm.2006.05.037.
[39] K. Jores, W. Mehnert, M. Drechsler, H. Bunjes, C. Johann, K. Mäder, Investigations on the structure of solid lipid nanoparticles (SLN) and oil-loaded solid lipid nanoparticles by photon correlation spectroscopy, field-flow fractionation and transmission electron microscopy, J. Contr. Release 95 (2) (2004) 217–227, https://doi.org/10.1016/j.jconrel.2003.11.012.
[40] E.I. Paramera, S.J. Konteles, V.T. Karathanos, Microencapsulation of curcumin in cells of Saccharomyces cerevisiae, Food Chem. 125 (3) (2011) 892–902, https://doi.org/10.1016/j.foodchem.2010.09.063.
[41] M.M. Yallapu, B.K. Gupta, M. Jaggi, S.C. Chauhan, Fabrication of curcumin encapsulated PLGA nanoparticles for improved therapeutic effects in metastatic cancer cells, J. Colloid Interface Sci. 351 (1) (2010) 19–29, https://doi.org/10.1016/j.jcis.2010.05.022.
[42] P. Dandekar, R. Dhumal, R. Jain, D. Tiwari, G. Vanage, V. Patravale, Toxicological evaluation of pH-sensitive nanoparticles of curcumin: acute, sub-acute and genotoxicity studies, Food Chem. Toxicol. 48 (2010) 2073–2089, https://doi.org/10.1016/j.fct.2010.05.008.
[43] M.M. Yallapu, M. Jaggi, S.C. Chauhan, Beta-Cyclodextrin-curcumin self-assembly enhances curcumin delivery in prostate cancer cells, Colloids Surf. B Biointerfaces 79 (1) (2010) 113–125, https://doi.org/10.1016/j.colsurfb.2010.03.039.
[44] S.P. Lacerda, N.N.P. Cerize, M.I. Ré, Preparation and characterization of carnauba wax nanostructured lipid carriers containing benzophenone-3, Int. J. Cosmet. Sci. 33 (4) (2001) 312–321, https://doi.org/10.1111/j.1468-2494.2010.00626.x.
[45] M. Iwata, S. Suzuki, Y. Asai, T. Inoue, K. Takagi, Involvement of nitric oxide in a rat model of carrageenin-induced pleurisy, Mediat. Inflamm. (2010) 682879, https://doi.org/10.1155/2010/682879, 2010.
[46] A.R. Moore, Pleural models of inflammation immune and nonimmune, Methods Mol. Biol. 225 (3) (2003) 123–128, https://doi.org/10.1385/1-59259-374-7:123.
[47] C.J. Morris, Carrageenan-induced paw edema in the rat and mouse, Methods Mol. Biol. 225 (2003) 115–121, https://doi.org/10.1385/1-59259-374-7:115.
[48] Y. Surh, Anti-tumor promoting potential of selected spice ingredients with antioxidative and anti-inflammatory activities : a short review, Food Chem. Toxicol. 40 (2002) 1091–1097, https://doi.org/10.1016/s0278-6915(02)00037-6.
[49] S. Kheradmandnia, E. Vasheghani-Farahani, M. Nosrati, F. Atyabi, Preparation and characterization of ketoprofen-loaded solid lipid nanoparticles made from beeswax and carnauba wax, Nanomedicine 6 (6) (2010) 753–759, https://doi.org/10.1016/j.nano.2010.06.003.
[50] H. Cai, Z. Zheng, Y. Sun, Z. Liu, M. Zhang, C. Li, The effect of curcumin and its nanoformulation on adjuvant-induced arthritis in rats, Drug Des. Dev. Ther. 9 (2015) 4931–4932, https://doi.org/10.2147/DDDT.S90147.